UNIVERSITY OF
BATH

*Citation for published version:*
Plummer, A & Lai, G 2015, 'New concepts for parallel kinematic mechanisms using fluid actuation' Paper
presented at 7th International conference on Fluid Power and Mechatronics, Harbin, China, 5/08/15 - 7/09/15, .

*Publication date:*
2015

*Document Version*
Early version, also known as pre-print

Link to publication

**University of Bath**

# New concepts for parallel kinematic mechanisms using fluid actuation

A R Plummer, G Lai

Centre for Power Transmission and Motion Control
Department of Mechanical Engineering
University of Bath, UK
A.R.Plummer@bath.ac.uk

*Abstract*—**Parallel kinematic mechanisms (PKMs), for example Stewart platforms, are widely used for high performance multi-axis motion systems. Their high stiffness and low mass are particularly suited to applications requiring good dynamic response, and the use of hydraulic actuators having exceptional power-to-weight ratio are also a good choice for such applications. Many configurations of PKMs have been built, including over-constrained systems with more actuators than degrees-of-freedom, but most are designed to move one rigid body with respect to another (ground). In this paper, generalized PKMs are discussed, involving the motion of multiple rigid bodies, typically within pre-stressed (i.e. overconstrained) actuator networks. Such systems could be used for morphing aircraft wings, lightweight actuated space structures, or in robotics. It is suggested that analytical techniques from the field of tensegrity structures can be used, where structural stability typically depends on geometric stiffness which results from pre-stressing.**

*Keywords—parallel kinematic mechanism, multi-axis control, tensegrity, overconstraint, morphing*

## I. INTRODUCTION

Many industries require machines which can dynamically control motion or force simultaneously in several linear or rotary axes. The testing and simulation industry is an example, where in-service motion or force usually needs to be replicated; this ranges from automotive durability testing, to earthquake simulation, and motion-based flight training simulators. Increasingly demanding applications are emerging for lightweight dynamic multi-axis motion control systems, such as for morphing aircraft wings, or high degree-of-freedom robot manipulators.

It is suggested in this discussion paper that there is potential for future multi-axis motion systems to achieve exceptional performance through integration of structures, actuation and control, and their mathematical optimization. Through the analysis of the complex static and dynamic characteristics of multi-element pre-stressed structures with distributed fluid actuation (e.g. Fig.1), it should be possible to derive synthesis rules to create the structural, actuation, sensing, and control design parameters to meet application-specific performance requirements. The aims are to achieve high stiffness, low weight, high speed of response, increased flexibility (i.e. allowing more degrees-of-freedom), and also redundancy if required. Modular systems which can be easily rebuilt into new configurations are also possible, as are machines with digitally controlled, massively distributed actuation.

## II. STATE-OF-THE-ART

### A. Actuated tensegrity structures

The proposed multi-axis systems configuration is a type of actuated tensegrity structure. Buckminster Fuller [1] coined the word tensegrity, conjoining tension and integrity, to mean structures consisting of members that are purely in compression (struts) stabilized by members that are purely in tension (cables). The structure is pre-stressed to ensure cables remain in tension in the presence of external forces, and hence the structure remains stiff. No member experiences a bending moment, which potentially allows an exceptionally good stiffness-to-mass ratio.

There is an increasing interest in tensegrity in the architecture and civil engineering fields; a good example is the Australian Kurilpa Bridge, a multiple-mast cable-stay structure built in 2009. The analysis of biological structures using tensegrity is another recent development. In the musculoskeletal system the muscles and connective tissues are the tensile members and the bones are the compressive struts [2].
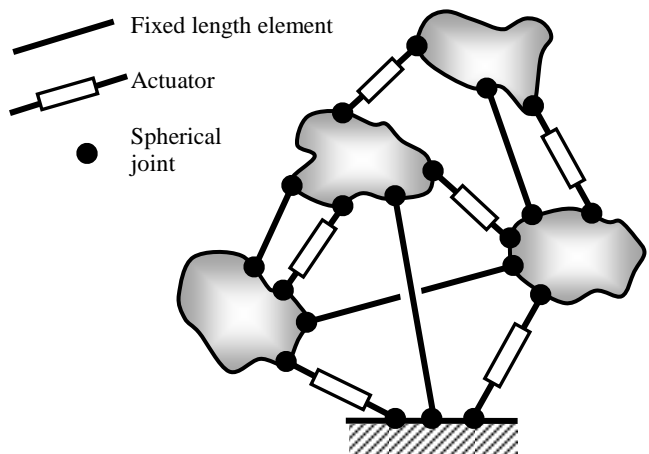


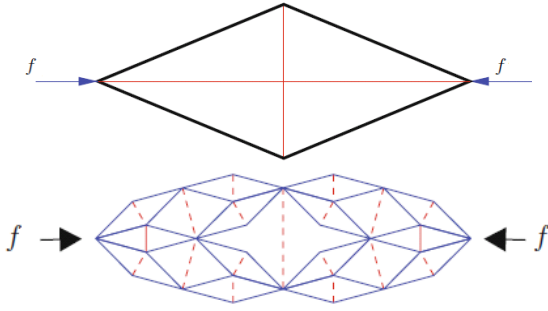Fig.1. Example PKM schematic with multiple bodies (nodes)

Fig. 2 Top: 'D-bar' tensegrity structure under compressive load (struts are bold lines). Bottom: Replacing D-bar struts with scaled-down D-bars, forming a tensegrity 'fractal' (axial cables not shown) [5]

Much of the scientific research on tensegrity structures concerns the form-finding problem: for a particular number of members (struts and cables) and their interconnections, find the set of member lengths and pre-stress which gives a stable structure [3,4]. These results are quite limited for engineering design, as amongst other factors the structure should have high strength and stiffness to mass ratios – just being stable is not sufficient. Useful analytical results for simple tensegrity structures giving optimum strength under compressive and bending loads are given by Skelton and de Oliveira in [5], although there is more work to do to consider engineering issues such as the fact that in reality several struts and cables cannot meet at a single point (i.e. the nodes where they meet have finite size: each is a rigid body in its own right). Nevertheless, the theoretical results indicate that a tensegrity structure under compression could have around half the mass of a conventional cylindrical strut, reducing in mass further if multiple scaled structures are used in a fractal-like configuration (Fig. 2). Deriving efficient methods for calculating structural stiffness of general tensegrity structures, in the form a stiffness matrix, has only reached maturity relatively recently [6].

The kinematics, dynamics and control of *actuated* tensegrity structures have received little attention due to their mathematical complexity, and the need to combine dynamics/control expertise with structural optimization. Experimental investigation in particular has been absent. The advantages of the concept have been explored most by Skelton at the University of California [5], who has analyzed dynamic properties and proposed controllers, but with limited experimental validation. For dynamic analysis, the struts are considered rigid, and the cables massless [5,7], and by using tension coefficients (tension divided by length of the member) as the input variables the equations of motion for the general nonlinear tensegrity system are found to have a bilinear structure. Control methods were first proposed for planar structures in 2003 [8]. A difficulty is that cables can only take tension, which is a type of control saturation, and complicates control design.

The concept of using tensegrity structures for wing morphing, mechanically actuated via cables running through the structure, is described in [9] and [10], but again this is theoretical only. Actuated tensegrity structures have also been proposed to create 'responsive architecture', for which

pneumatic actuation has been suggested, but scientific details have not been published [11]. There are no other examples of fluid-actuated tensegrity structures in the literature, but some are now being built at the University of Bath (Fig 3).

An interesting concept for a planetary exploration rover has emerged from NASA, using an actuated tensegrity structure to provide locomotion through its changes of shape [12,13]. It effectively rolls over the ground (Fig. 4).

Existing research into the dynamics and control of more conventional parallel kinematic machines using fluid actuation can be extended to the proposed structures. In particular, existing methods for controlling internal forces (pre-stress) in such machines can be used [14], and the benefits of modal decomposition – closing the loop in modal coordinates – allowing resonant modes to be decoupled still applies [15].
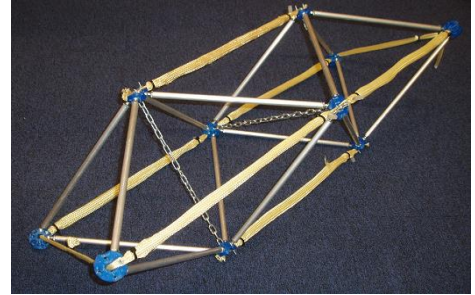


Fig.3. Tensegrity structure actuated using McKibben 'pneumatic muscles' at the University of Bath
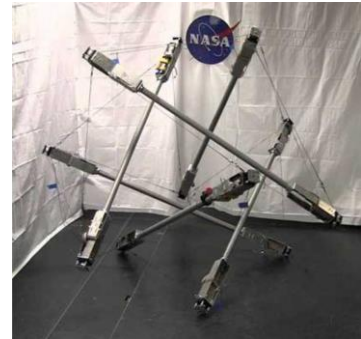


Fig. 4. NASA 'Superball' tensegrity robot platform [12,13]

### B. Application example: morphing aircraft wings

Using actuated tensegrity structures, aircraft wings and other aerodynamic surfaces will be able to change shape by distributing actuation throughout the wing structure (morphing), eradicating the need for separate control surfaces. According to NASA: "Aircraft of the future will not be built of traditional, multiple, mechanically connected parts and systems. Instead, aircraft wing construction will employ fully-integrated, embedded 'smart' materials and actuators that will enable aircraft wings with unprecedented levels of aerodynamic efficiencies and aircraft control."[16].

The traditional method of aircraft control relies on the deflection of hinged, discrete control surfaces, which can, even under moderate levels of deflection, set up localised areas of severe adverse pressure gradient (typically along the

hinge line) that produce regions of flow separation, and poor wing efficiency. Morphing allows subtle changes in curvature, leading to better aerodynamic performance. However the morphing concept has not been commercialised as previously an effective active structure solution to achieve morphing has not been found [17].

## C. Application example: human friendly robots

More robots in the future will need to share an environment with humans, e.g. in domestic, entertainment, assistive or medical applications. They must fulfil different requirements from those typically met in industry, so conventional industrial arms are not appropriate. Making a rigid, heavy robot behave gently and safely is not generally possible [18,19]. The most successful design to date, the DLR arm, has focused on minimising inertia [20]. Another approach to increasing the safety level of robot arms interacting with humans is to intentionally introduce mechanical compliance in the design, however compliant transmissions introduce resonances and loss of positional accuracy. An actuated tensegrity structure, integrating lightweight fluid actuation within an optimized configuration, provides an ideal approach to create an ultra-lightweight arm. Although never pursued, using tensegrity (but not fluid actuation) for human-friendly robots was first proposed in 2003 at the University of California: "...bandwidth can also be recovered by reducing system mass. For instance, the tensegrity systems can be designed with exceptionally low system mass ... The work herein suggests that tensegrity concepts will revolutionize the manner in which tendon-driven systems are designed, controlled and utilized. We believe this will become especially true in environments where agile manoeuvring and delicate object handling require a 'soft' touch" [8].

## D. Other possible applications

Snake-arm robots are slender manipulators with many joints, designed to perform remote handling operations in confined and hazardous spaces [21]. They can fit through small openings and reach around obstacles. With the problems of radiation dosage and confined spaces, the nuclear industry has been driving the development of these manipulators [22,23]. In the aerospace industry, there is a desire to adopt automation in order to increase throughput and standardize processes. However, it is nearly impossible to use a conventional industrial robot-arm to pass through an access hole, for example, and conduct work within a wing box, and so research is progressing on snake arm robots to do this task. There are other potential applications in confined spaces in mining and process industries for repair and maintenance, and a suggested medical application is minimally-invasive surgery [24].

Snake-arm robots are tendon driven arms with wires terminating in different segments along the length of the arm. Thus the number of segments is limited, and cable friction and cable stretch are technical challenges. It is proposed that a fluid-actuated tensegrity structure is an alternative solution which does not have these drawbacks.

Other applications include deployable, adaptive space structures, and structures requiring distributed vibration isolation/damping. Large, lightweight truss-type space structures are increasingly used to support antennae and instrumentation. Actuated tensegrity structures provide the opportunity for changing the positioning of instruments, and for active damping of the low resonant modes.
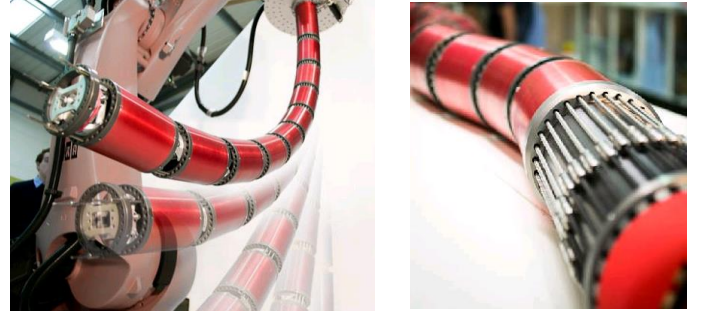


Fig.5 The first commercial snake arm robot (www.ocrobotics.com)

## III. STRUCTURE GEOMETRY AND STABILITY

### A. Finding equilibrium node positions

Consider a pin jointed structure such as that shown in Fig. 6. There are $n$ nodes (in this case 10) and $m$ structural members (in this case 27). As it is pin jointed, the members experience no bending moment. Typically, each member is designed to support either a compressive load (in which case it is called a strut), or a tensile load (in which case it is called a cable). Struts a depicted with thicker lines. In general, the structure is pre-stressed; this is often necessary to keep the force in the right direction (tension or compression) in the cables and struts when the structure is supporting an external load, and may be necessary to stabilize the structure via its resulting geometric stiffness (discussed later). In the following, the stiffness of each member is specified, and an
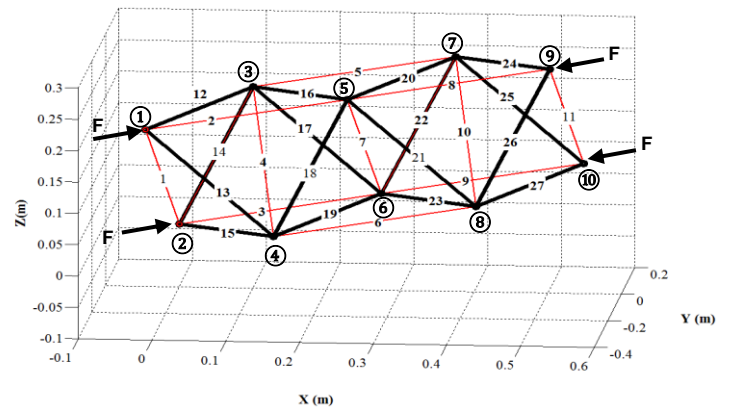


Fig. 6. Example tensegrity structure (struts are thick lines)

iterative approach is used move the node positions until the resultant force at each node reaches zero. The resulting node positions (if they exist) are those for the structure in static equilibrium. This calculation can be carried out either with or without external loads applied to nodes in the structure (in the example of Fig. 6 external load $F$ is applied to four nodes).

The configuration of the structure is defined by its connectivity matrix, $\mathbf{C} \in \mathfrak{R}^{m \times n}$, where there is one row for each member and each row contains a -1 and a +1 indicating the two nodes which the member spans, and otherwise the elements are zero. For example, the first four rows (members) for the structure of Fig. 6 are:

$$\mathbf{C} = \begin{bmatrix} -1 & 1 & 0 & 0 & 0 & \cdots \\ -1 & 0 & 0 & 0 & 1 & \cdots \\ 0 & -1 & 0 & 0 & 0 & \cdots \\ 0 & 0 & -1 & 1 & 0 & \cdots \\ \vdots & \vdots & \vdots & \vdots & \vdots & \ddots \end{bmatrix} \quad (1)$$

Let $\mathbf{N} \in \mathfrak{R}^{3 \times n}$ be a matrix of node coordinates:

$$\mathbf{N} = \begin{bmatrix} \mathbf{x} \\ \mathbf{y} \\ \mathbf{z} \end{bmatrix} \quad (2)$$

where $\mathbf{x} = \begin{bmatrix} x_1 & x_2 & \cdots & x_n \end{bmatrix}$, $\mathbf{y} = \begin{bmatrix} y_1 & y_2 & \cdots & y_n \end{bmatrix}$ and $\mathbf{z} = \begin{bmatrix} z_1 & z_2 & \cdots & z_n \end{bmatrix}$. Representing each member by a vector (from its '-1' node to its '+1' node), the matrix of member vectors $\mathbf{M} \in \mathfrak{R}^{3 \times m}$ is given by:

$$\mathbf{M} = \mathbf{N}\mathbf{C}^T \quad (3)$$

A vector $\mathbf{l_m} \in \mathfrak{R}^{m \times 1}$ of member lengths can be calculated from $\mathbf{M}$, each element being:

$$l_{mi} = \sqrt{\mathbf{m_i}^T \mathbf{m_i}} \quad (4)$$

where $\qquad \mathbf{m_i} = \begin{bmatrix} \mathbf{M}(1,i) & \mathbf{M}(2,i) & \mathbf{M}(3,i) \end{bmatrix}^T \quad (5)$

Let the vector of free (unloaded) member lengths be $\mathbf{l_{m0}}$, so the tension in each member is given by:

$$\mathbf{f_m} = \mathbf{K_m}(\mathbf{l_m} - \mathbf{l_{m0}}) \quad (6)$$

where $\mathbf{K_m} \in \mathfrak{R}^{m \times m}$ is a diagonal matrix of the member stiffnesses. Projecting these forces along the member vectors contained in $\mathbf{M}$ gives the matrix of member force vectors $\mathbf{F_m} \in \mathfrak{R}^{3 \times m}$:

$$\mathbf{F_m} = \mathbf{M}\,\mathrm{diag}(\begin{bmatrix} f_{m1}/l_{m1} & \cdots & f_{mi}/l_{mi} & \cdots & f_{mm}/l_{mm} \end{bmatrix}) \quad (7)$$

where diag() is a diagonal matrix with its vector argument providing the sequence of leading diagonal elements. Force vectors of positive magnitude in $\mathbf{F_m}$ (i.e. tension) point from the '-1' to the '+1' nodes defined in $\mathbf{C}$.

The matrix $\mathbf{F_n} \in \mathfrak{R}^{3 \times n}$ of resultant force vectors at each node is given by:

$$\mathbf{F_n} = -\mathbf{F_m}\mathbf{C} + \mathbf{F_e} \quad (8)$$

where $\mathbf{F_e} \in \mathfrak{R}^{3 \times n}$ is the matrix of node external force vectors (zero for a structure with no externally applied loads). The external forces must be specified to give a zero resultant force and moment on the structure.

Now consider the stiffness matrix $\mathbf{K_n} \in \mathfrak{R}^{3n \times 3n}$ which relates node displacements in each Cartesian direction to the corresponding change in node forces. Express the node position coordinates in one vector $\mathbf{n_v} \in \mathfrak{R}^{3n \times 1}$ and the node force vectors similarly in $\mathbf{f_v} \in \mathfrak{R}^{3n \times 1}$:

$$\begin{aligned} \mathbf{n_v} &= \begin{bmatrix} \mathbf{x} & \mathbf{y} & \mathbf{z} \end{bmatrix}^T \\ \mathbf{f_v} &= \begin{bmatrix} \mathbf{F_n}(1,1) & \mathbf{F_n}(1,2) & \cdots & \mathbf{F_n}(2,1) & \cdots & \mathbf{F_n}(3,1) & \cdots \end{bmatrix}^T \end{aligned} \quad (9)$$

The node stiffness matrix relates small changes in these vectors:

$$\Delta\mathbf{f_v} = \mathbf{K_n}\Delta\mathbf{n_v} \quad (10)$$

How to find $\mathbf{K_n}$ is discussed later.

The stiffness matrix can be diagonalized by transforming the displacements and forces into a modal co-ordinate system. A linear transformation is given by:

$$\Delta\mathbf{n_m} = \mathbf{P}^{-1}\Delta\mathbf{n_v} \qquad \Delta\mathbf{f_m} = \mathbf{P}^{-1}\Delta\mathbf{f_v} \quad (11)$$

where $\mathbf{P} \in \mathfrak{R}^{3n \times 3n}$, giving:

$$\Delta\mathbf{f_m} = \mathbf{P}^{-1}\mathbf{K_n}\mathbf{P}\Delta n_m \quad (12)$$

or $\qquad\qquad \Delta\mathbf{f_m} = \mathbf{\Omega}\Delta\mathbf{n_m} \quad (13)$

where $\mathbf{P} \in \mathfrak{R}^{3n \times 3n}$ is a diagonal matrix. If $\mathbf{P}$ has as its columns the eigenvectors of $\mathbf{K_n}$, then this diagonalization is achieved, and the elements on the diagonal of $\mathbf{\Omega}$ are the eigenvalues of $\mathbf{K_n}$ (which are the 'modal stiffnesses').

A stable set of node positions, if it exists, can be found by iterating a set of trial positions until the resultant force at each node is zero. The change in node position at each iteration will be that which changes the resultant forces to zero according to the latest stiffness matrix; iteration is required as the stiffness matrix varies with position.

$$\mathbf{n_m}(i+1) = \mathbf{n_m}(i) - \mathbf{\Omega}'(i)\mathbf{f_m}(i) \quad (14)$$

The matrix $\mathbf{\Omega'} \in \Re^{3n \times 3n}$ is a modified inverse of $\mathbf{\Omega}$. Ordering the modal stiffness values (diagonal elements) in $\mathbf{\Omega}$ and the columns in $\mathbf{P}$ correspondingly:

$$\mathbf{\Omega} = \mathrm{diag}([\lambda_1 \quad \lambda_2 \quad \ldots \quad \lambda_{3n}]) \tag{15}$$

where $|\lambda_k| > |\lambda_{k+1}|$, then:

$$\mathbf{\Omega'} = \mathrm{diag}([1/\lambda_1 \quad \cdots \quad 1/\lambda_{3n-6} \quad 0 \quad \cdots \quad 0]) \tag{16}$$

This inverse removes the six rigid body modes which have stiffness values $\lambda_k$ of zero, i.e. modes in which all nodes translate or rotate together without altering their relative position to one another. These modes are not relevant to altering the internal forces on the nodes.

Equation (13) can be used to iterate the node positions until some measure combining the resultant forces at all nodes (for example mean square value) is zero to within a chosen tolerance.

### B. Calculating the stiffness matrix

The movement of a single node in any direction will in general produce a change in force in all members connected to that node, thus changing the resultant force acting on the node and all nodes to which it is connected. These changes in node force are due not only to the change in magnitude of the member forces, but also their change in direction. The node stiffness due to member force magnitude change, which is dependent on the member stiffness, is the *elastic stiffness*. The node stiffness due to the member force direction change, which is dependent on the size of the member force but not its stiffness, is called the *geometric stiffness*.

The stiffness matrix can be determined from the derivative of a member force vector with respect to a node position vector, relating the member force back to the forces on the two nodes it interconnects, and summing the contributions for all members connected to each node. In this way it can be shown that the stiffness matrix is given by the following equations [6].

Let $\mathbf{J} \in \Re^{3n \times m}$ be the Jacobian which relates the rate of change of member lengths to the rate of change of node positions:

$$\mathbf{J} = \begin{bmatrix} \mathbf{C}^{\mathbf{T}} \mathrm{diag}(\mathbf{Cx}^{\mathbf{T}}) \mathrm{diag}([1/l_{m1} \quad \cdots \quad 1/l_{mm}]) \\ \mathbf{C}^{\mathbf{T}} \mathrm{diag}(\mathbf{Cy}^{\mathbf{T}}) \mathrm{diag}([1/l_{m1} \quad \cdots \quad 1/l_{mm}]) \\ \mathbf{C}^{\mathbf{T}} \mathrm{diag}(\mathbf{Cz}^{\mathbf{T}}) \mathrm{diag}([1/l_{m1} \quad \cdots \quad 1/l_{mm}]) \end{bmatrix} \tag{17}$$

remembering that $l_{mi}$ is the length of member $i$. The product of the diagonal matrices in each term of equation (17) gives the x, y and z components of the unit direction vectors of the members. The elastic stiffness $\mathbf{K_e} \in \Re^{3n \times 3n}$ at the nodes is given by:

$$\mathbf{K_e} = \mathbf{J} \, \mathrm{diag}([k_1 \quad \cdots \quad k_m]) \mathbf{J}^{\mathbf{T}} \tag{18}$$

where $k_i$ is the stiffness of member $i$. Let $\mathbf{q} \in \Re^{m \times 1}$ be a vector of member tension coefficients (sometimes called force densities), defined as:

$$\mathbf{q} = [f_{m1}/l_{m1} \quad \cdots \quad f_{mi}/l_{mi} \quad \cdots \quad f_{mm}/l_{mm}]^T \tag{19}$$

Then the geometric stiffness $\mathbf{K_g} \in \Re^{3n \times 3n}$ at the nodes is [5,6]:

$$\mathbf{K_g} = \mathbf{I_3} \otimes (\mathbf{C}^{\mathbf{T}} \mathrm{diag}(\mathbf{q})\mathbf{C}) - \mathbf{J} \, \mathrm{diag}(\mathbf{q}) \mathbf{J}^{\mathbf{T}} \tag{20}$$

where $\mathbf{I_3} \in \Re^{3 \times 3}$ is an identity matrix and $\otimes$ is the Kronecker product (thereby the first of the pair of terms in (20) is a block diagonal matrix with the $\mathbf{C}^{\mathbf{T}} \mathrm{diag}(\mathbf{q})\mathbf{C}$ block repeated 3 times). And the node stiffness is:

$$\mathbf{K_n} = \mathbf{K_e} + \mathbf{K_g} \tag{21}$$

### C. Extension to finite nodes

In general, a structure with several members meeting at each node (such as in Fig. 6) cannot be built in reality, requiring infinitesimally small pin joints. A physically realisable arrangement is for nodes to have finite dimensions, and for members to connect to nodes at joints separated in space from one another. Thus the practical arrangement is like the example in Fig. 1. A node with finite dimensions has 3 additional rotary degrees of freedom, and member stiffnesses and forces both contribute to the torsional stiffness in these directions. The node material itself will be assumed to be rigid in this paper.

The derivation is not included here, but the principle is that the previous iterative approach can be extended to include node rotation. Now the stiffness matrix $\mathbf{K_n} \in \Re^{6n \times 6n}$ relates both node translations and rotations to the corresponding change in node forces and moments. The node linear/angular position coordinates are expressed in one vector $\mathbf{n_v} \in \Re^{6n \times 1}$ and the node force/moment vectors similarly in $\mathbf{f_v} \in \Re^{6n \times 1}$. Thus:

$$\mathbf{n_v} = [\mathbf{x} \quad \mathbf{y} \quad \mathbf{z} \quad \boldsymbol{\varphi} \quad \boldsymbol{\theta} \quad \boldsymbol{\psi}]^T \tag{22}$$

where the three orthogonal rotations are roll $\boldsymbol{\varphi} \in \Re^{1 \times n}$, pitch $\boldsymbol{\theta} \in \Re^{1 \times n}$ and yaw $\boldsymbol{\psi} \in \Re^{1 \times n}$ Euler angles

Now, member lengths (equations 3 and 4) have to be calculated including the orientation of the nodes, and the member forces are combined not only to give a resultant force on each node (equation 8) but also a resultant moment. Other than dimensions, the diagonalisation and iteration equations are just the same as before (equations 11 to 16).

## IV. EXAMPLE ACTUATED STRUCTURE

Fig. 7 shows plan and side views of a structure with 13 struts, 20 cables and 12 nodes (looking in negative Z and X directions respectively). The members do not meet at a point, i.e. the nodes have finite size. The circles indicate pin joints; the bodies of the nodes are not shown. Fig. 8. is an isometric view of the same structure.

Consider the case where four tension members (cables) in the central part of the structure are actuated (members 15, 18, 21 and 24). These can be controlled antagonistically to generate three independent motions, whilst also controlling the tension in the structure.

Contracting members 15 and 18 by 15%, and extending members 21 and 24 by 20% causes the bend in the XY plane shown in Fig. 9 (compare with top view in Fig. 7). Alternatively, contracting members 15 and 24 and extending members 18 and 21 causes the shear motion in the YZ plane shown in Fig 10 (compare with bottom view in Fig. 7). The third motion, contracting (or extending) members 18 and 24 and extending (or contracting) members 15 and 21 causes a motion approximating to a twist about the Y axis.
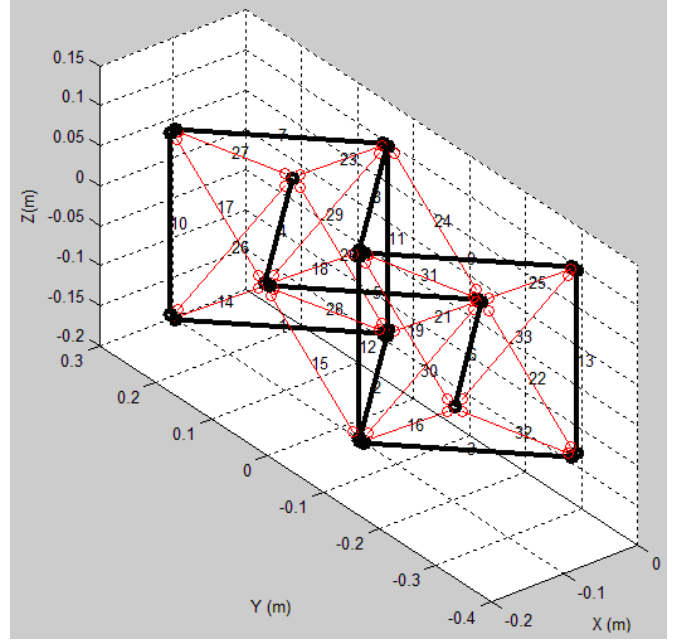


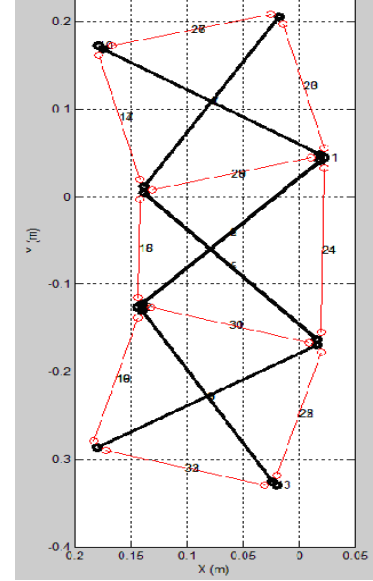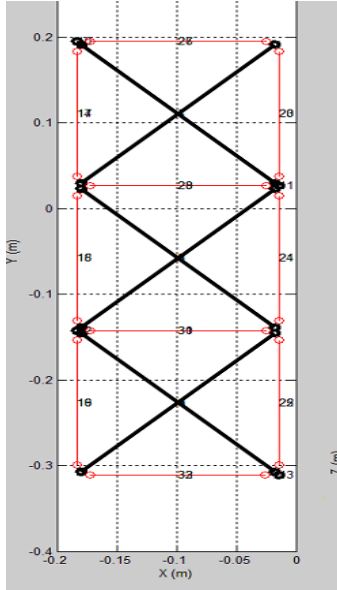Fig. 8  Same example structure, isometric view



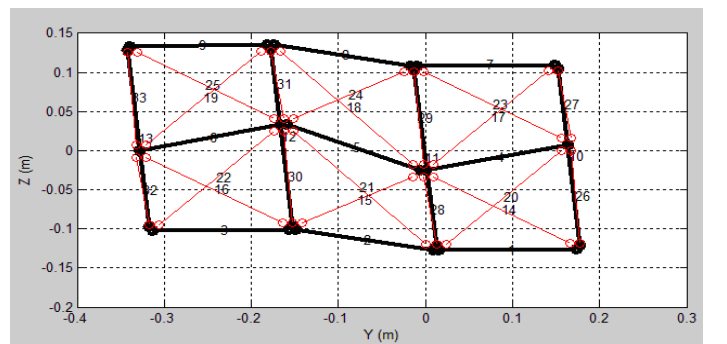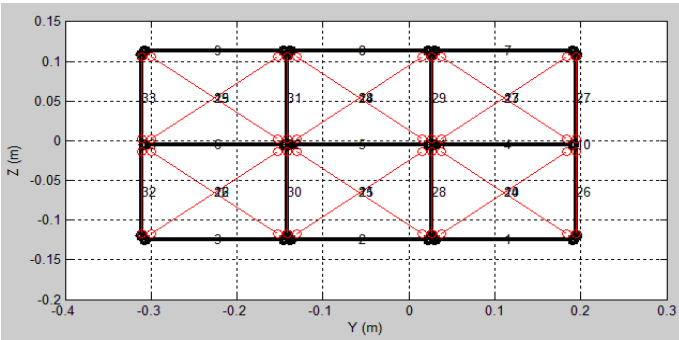Fig. 9.  Bending displacement (contracting 15 and 18, extending 21 and 24)



Fig. 7.  Example structure with finite node dimensions (plan and side view)



Fig. 10.  Shear displacement (contracting 15 and 24, extending 18 and 21)

## V. Control

A combination of position and internal force control is necessary in order to achieve the desired motion whilst maintaining an appropriate level of pre-stress. It is assumed that the actuator forces are measured, forming vector $\mathbf{f_a} \in \Re^{a \times 1}$ (the number of actuators being $a$), which is thus a subset of $\mathbf{f_m}$. Also the actuator displacements away from their nominal zero positions are measured giving vector $\delta_\mathbf{a} \in \Re^{a \times 1}$. These feedback signals need to be combined to form virtual feedbacks $\mathbf{f_d} \in \Re^{(a-d) \times 1}$ and $\delta_\mathbf{c} \in \Re^{d \times 1}$ as shown in Fig. 11, where $d$ is the number of independent degrees-of-freedom. Thus transformation $\mathbf{P}$ defines the workspace position co-ordinates. $\mathbf{P}$ and the other signal transformations in Fig. 11 could be based on full kinematic models, or they could be constant linear matrix transformations if displacements are small. Assuming the latter, then: $\mathbf{P} \in \Re^{d \times a}$, $\mathbf{U} \in \Re^{a \times d}$, $\mathbf{D} \in \Re^{a \times (a-d)}$, and $\mathbf{Q} \in \Re^{(a-d) \times a}$. The compensators, which might just be proportional-integral controllers, are implemented in workspace co-ordinates.

The choice of $\mathbf{P}$, defining the workspace control co-ordinates, depends on user requirements. It could simply be a set of actuator position differences, which for the example in Section IV (with $a$=4 and $d$=3) might be:

$$\mathbf{P} = \begin{bmatrix} -1 & -1 & 1 & 1 \\ -1 & 1 & -1 & 1 \\ -1 & 1 & 1 & -1 \end{bmatrix} \qquad (23)$$

and the conversion of the position loop control signal components back to actuator co-ordinate space can be achieved by $\mathbf{C} = \mathbf{P}^T$.

As derived in [14], the columns of $\mathbf{D}$ should form the basis of the null space of $\mathbf{P}$, and a suitable choice for $\mathbf{Q}$ is $\mathbf{Q} = \mathbf{D}^T$. In this case:

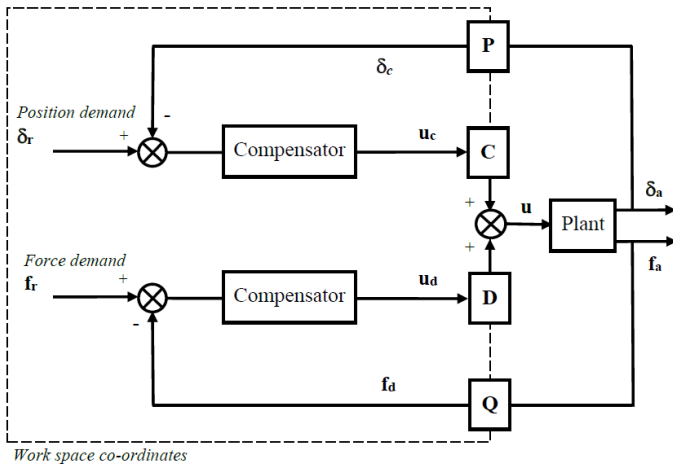$$\mathbf{Q} = \begin{bmatrix} 1 & 1 & 1 & 1 \end{bmatrix} \qquad (24)$$



Fig. 11 Multi-axis control scheme (modified from [14])

In this example it is clear how the actuators act antagonistically against one another to produce motion, but in a more complex structure this may not be so, and not all actuators will contribute to all degrees-of-freedom. More fundamentally, determining the number of degrees-of-freedom of the structure and solving the kinematic equations are complex tasks, and require research. The use of screw theory is a way to formulate the problem which may simplify the task [25, 26].

## VI. Conclusions

Future dynamic machines will require distributed actuation integrated with load-bearing structures, so that they are lighter, move faster, use less energy, are more human-friendly, and are more adaptable. Good examples are shape-changing aircraft wings which can adapt precisely to the ideal aerodynamic form for current flying conditions, and light but powerful human-friendly robotic manipulators which can interact safely with human co-workers.

To achieve this, a new type of parallel kinematic mechanism is proposed which is a multi-element pre-stressed structure with distributed fluid actuation. There are strong parallels with high performance motion systems found in nature, such as the musculo-skeletal system in vertebrates. The performance levels of these biological systems are much better than man-made machines. Development of these new mechanisms will utilize expertise in kinematics, dynamics, hydraulic actuation, and multi-axis motion control, combined with results from the field of tensegrity structures.

It is shown in this paper that tensegrity structures, with practical nodes of finite dimension, can be designed with actuated members to give shape changing properties. Static tensegrity structures can be engineered so that member forces always intersect at a point at each node, and any small dimensional errors can be accommodated by having built-in rather than pin-jointed members; shape-changing structures do not have this luxury. As a general rule, cables (tensile members) stabilize a finite node by contributing positive geometric stiffness, while struts destabilize, causing twisting of the node (buckling the load path). Thus the former must be designed always to dominate the latter. Specific research issues are:

- the development of mathematical techniques to analyze a given structure in terms of measures of specific stiffness, and strength.

- finding efficient methods to calculate and express shape change forward kinematics (change in length of actuated members to change in node positions).

- deriving techniques to synthesize structures to meet given specifications

- establishing methods to determine dynamic models suitable for controller design.

- proposing and validating control schemes to provide closed-loop motion and/or force control, including

internal force (pre-stress) control and handling redundancy.

- using a systems engineering approach to maximize closed-loop performance, by adjusting the structural parameters in conjunction with the controller parameters (for example trade-offs between inherent structural stiffness and closed loop stiffness).

## REFERENCES

[1] Fuller,R.B. (1959) Tensile integrity structures. US patent 3.063.521.

[2] Levin, S. (2006) "Tensegrity, The New Biomechanics"; Hutson, M & Ellis, R (Eds.), Textbook of Musculoskeletal Medicine. Oxford University Press

[3] Tran, H., Lee, J. (2013) Form-finding of tensegrity structures using double singular value decomposition. Engineering with Computers (2013) 29:71–86

[4] Koohestani, K., Guest, S. D. (2013). A new approach to the analytical and numerical form-finding of tensegrity structures. Int J of Solids and Structures, 50(19).

[5] Skelton, R.E., de Oliveira, M.C. (2009) Tensegrity Systems. Springer, Boston.

[6] Guest,S (2006) The stiffness of pre-stressed frameworks: A unifying approach. Int J of Solids and Structures 43.

[7] Skelton, R E (2005). Dynamics and control of tensegrity systems. Proc IUTAM Symposium on Vibration Control of Nonlinear Mechanisms and Structures, Munich.

[8] Aldrich, J, R. E. Skelton, and K. Kreutz-Delgado. (2003) Control synthesis for a class of light and agile robotic tensegrity structures. Proc. American Control Conference,Denver.

[9] Moored, K.W. and H. Bart-Smith (2007) The analysis of tensegrity structures for the design of a morphing wing. Journal of Applied Mechanics - Transactions of the ASME, 74(4).

[10] Moored, K.W. and H. Bart-Smith (2009) Investigation of clustered actuation in tensegrity structures. Int J. of Solids and Structures, 2009. 46(17).

[11] Sterk, T (2003) Using Actuated Tensegrity Structures to Produce a Responsive Architecture. Proc ACADIA22, Ball State University.

[12] J.,Bruce, K. Caluwaerts, A. Iscen, A. P. Sabelhaus, & V. SunSpiral, Design and evolution of a modular tensegrity robot platform. In Robotics and Automation (ICRA), 2014 IEEE International Conference on (pp. 3483-3489).IEEE, 2014.

[13] Spectrum.ieee.org, „NASA's Super Ball Bot Could Be the Best Design for Planetary Exploration - IEEE Spectrum", 2015. [Online]. http://spectrum.ieee.org/automaton/robotics/military-robots/nasa-super-ball-bot.

[14] Plummer, A. R. (2010) A general co-ordinate transformation framework for multi-axis motion control with applications in the testing industry Control Engineering Practice. 18, 6.

[15] Plummer, A. R. & Guinzio, P. S (2009) Modal control of an electrohydrostatic flight simulator motion system. Proc ASME Dynamic Systems and Control Conference 2009, Los Angeles

[16] http://www.nasa.gov/centers/Langley/news/factsheets /21stcentury.html (29/09/14)

[17] Valasek J (Ed) (2012) Morphing Aerospace Vehicles and Structures. Wiley, Chichester.

[18] Bicchi, A, Tonietti, G (2004) Dealing with the Safety-Performance Tradeoff in Robot Arms Design and Control. IEEE Robotics & Automation Magazine, June 2004.

[19] Salisbury, K. et al (1988) Preliminary design of a whole-arm manipulation system (WAMS), Proc.1988 IEEE Int. Conf. Robot. Automat., Philadelphia.

[20] Haddadin, S., Albu-Schäffer,A., Hirzinger, H., (2010) Safety Analysis for a Human-Friendly Manipulator. Int J Soc Robot (2010) 2: 235–252

[21] He, J, Liu, R, Wang ,K, Shen, H (2012) The mechanical design of snake-arm robot. 10th IEEE International Conf. on Industrial Informatics (INDIN).

[22] Bloss, R. "Robotic Snake Arm Reaches Into Radioactive Regions", Industrial Robot, Volume 38, Number 2, p200-201

[23] Buckingham, R, Graham,A, (2005) Snaking around in a nuclear jungle Int. J. Industrial Robot, Vol. 32, No. 2

[24] Zenati, M, T. Yokota, D. Schwartzman, T. Ota, B. Zubiate, C. Wright, C. Nikou, and H. Choset (2010) Model-Guided Single Port Epicardial Interventions Using a Highly Articulated Robotic System. Proc of the Minimally Invasive Robotic Association Fifth International Congress, San Diego

[25] Hunt, K.H., (1978) Kinematric Geometry of Mechanisms. Oxford University Press, London.

[26] Dai, J.S., Huang, Z., Lipkin, H. (2006) Mobility of Overconstrained Mechansims. Transactions of the ASME, J of Mechanical Design, Vol 128, p220-229.